TURBULENT STRIPE SURVIVAL IN PLANE COUETTE FLOW

Hirohito Kawajiri
Department of Mechanical Engineering,
Doshisha University, 1-3 Tatara
Miyakodani, Kyotanabe-shi, Kyoto, Japan
ctwg0532@mail4.doshisha.ac.jp

Koji Fukudome
Department of Mechanical Engineering,
Tokyo University of Science, 6-3-1
Niijuku, Katsushika-ku, Tokyo, Japan
kfukudome@rs.tus.ac.jp

Shumpei Hara
Department of Mechanical Engineering,
Doshisha University, 1-3 Tatara
Miyakodani, Kyotanabe-shi, Kyoto, Japan
shhara@mail.doshisha.ac.jp

ABSTRACT

In this study, visualization experiments of plane Couette flow were conducted to investigate the spatio-temporal characteristics of the angle against the streamwise direction (θ), the number of turbulent bands generated in the subcritical transition regime, and the survival time of turbulent stripes. The experiment was conducted with different film half-widths (δ). The appearance and decay of two cycles of turbulent stripes were captured at visualized times of Reynolds number of 300 and 330, and named the long-life and short-life cycles in the order of their appearance. There were differences in the angle of turbulent stripes and turbulent bands in each cycle. In the long-life cycle, one turbulent band was characterized at a maximum θ of 40° to the streamwise direction for small δ, with a survival time of t^* = 1620. For the large δ, one turbulent band was characterized at a maximum θ of 35°, with a survival time of t^* = 1960. In the short-life cycle, five turbulent bands were characterized at a maximum θ of 20° to the streamwise direction for small δ, with a survival time of t^* = 970. For the large δ, one turbulent band was characterized at a maximum θ of 37°, with a survival time of t^* = 1240. In the long-life cycle, similar angles of turbulent stripes were observed for each δ. On the other hand, a larger angle was observed for the short-life cycle with large δ. The number of turbulent bands of each cycle was found to be much for small δ. The survival time of turbulent stripes depends on the angle of the turbulence stripes, and θ = 35° was found to have the longest survival time at t^* = 1960. The experimental results in this study showed that the value of spanwise wavelength was different for small and large δ.

INTRODUCTION

Turbulent stripe appears in the subcritical transition regime of a plane Couette flow, which is one of the canonical flows. Turbulent stripes are an intermittent structure in which a turbulent region with high velocity fluctuation and a quasi-laminar region with low velocity fluctuation are alternately arranged in the streamwise direction to form a stripe-like pattern (Prigent *et al.*, 2003). The study of the subcritical transition regime is important for low-Reynolds number heat exchangers (Fukudome *et al.*, 2018; Fukuda *et al.*, 2020). As industrial products become smaller and smaller, the flow paths become narrower and the Reynolds number becomes low-Reynolds number. It is difficult to sustain turbulence under low-Reynolds number, and it is important to clarify the critical Reynolds number at which turbulence can be maintained. Clarification of the mechanism of turbulent stripe in the subcritical transition will lead to efficient transport of materials.

It was reported that turbulent stripes appear for $325 \leq Re \leq 415$ (Manneville, 2004). Here, the Reynolds number is defined by the velocity of movement of both walls U_w, the film half-width δ and the kinematic viscosity ν. Subsequent studies (Barkley *et al.*, 2005; Reetz *et al.*, 2019) have reported the same Re range of turbulent stripe appearance.

The following three reports of turbulent stripes in a plane Poiseuille flow are introduced below. Hashimoto *et al.* (2009) reported in visualization experiments that the angle was 20° to 30°. Paranjape *et al.* (2020) succeeded in capturing the growth process and splitting of a single turbulent stripe generated in the subcritical transition regime by experiment. Fukudome *et al.* (2015) reported numerically that when the angle of the turbulent stripe is larger than 40°, high-and-low-speed streaks in the large scale are not maintained and the turbulent stripe structure decayed. Compared to Poiseuille flow, plane Couette flow generates turbulent energy only in the streamwise direction due to the constant shear deformation, and the turbulence is strongly anisotropic. Therefore, the growth process of the turbulent stripe is estimated to be different from that reported for the channel flow.

Plane Couette flow requires an even larger area than plane Poiseuille flow. Turbulent stripes have been observed at very large aspect ratios. Prigent *et al.* (2003, 2005) simultaneously visualized five turbulent bands within the visualization area under the condition of δ = 3.00 mm in the plane Couette flow. Gomé *et al.* (2020) captured the split and decay of turbulent stripes by extracting regions in a certain streamwise direction, and arranging them over time in a numerical simulation using the plane Couette flow. In this study, the spatio-temporal characteristics of turbulent stripes, such as angle against the streamwise direction, spanwise wavelength, and the number of bands, as well as the survival time of the turbulent stripes themselves, are of interest for understanding the phenomenon.

In this study, the film half-width differs from that of Prigent *et al*. (2003), visualization experiments of the plane Couette flow were conducted to investigate the spatio-temporal characteristics of the appearing turbulent stripes and their formation and decay processes (survival time), comparing them with previous studies on plane Couette flow and plane Poiseuille flow.

EXPERIMENTAL SET-UP

Figure 1 shows a schematic diagram of the experimental apparatus for the plane Couette flow. The experimental apparatus used in this study is similar to that utilized by Couliu *et al*. (2015). Equipment in Fig. 1 was submerged in a water tank ($1000\times1660\times300$ mm^3) filled with water and driven by a motor at a constant speed to form a plane Couette flow. A seamless cylindrical film was utilized to prevent disturbance to the flow. The film was adjusted to be stretched evenly. To verify the uniformity of the film half-width, the ranged measurement (green area in Fig. 1) was divided into nine square blocks. The film half-width at the center of each block was measured using a laser pointer and an acrylic cube. In this study, two experiments were conducted with different film half-widths. In the first experiment, the mean value for the nine film half-widths was 3.39 mm, with a standard deviation of 0.27 mm. To estimate the kinematic viscosity, thermometers were inserted into four corner points in the tank, and the average value of 288 K was used. In the second experiment, the film half-width was 2.90 mm, its standard deviation was 0.26 mm, and the water temperature was 297 K. In this study, the Reynolds number was lowered gradually from 450 and finally to 260. To visualize the flow, flake particles were inserted into the tank, and after confirming that the flow became steady at each Reynolds number, the flow was captured by a camera for 5 minutes.

CHARACTERISTICS OF ONE TURBULENT BAND

Figure 2 shows the images at Reynolds numbers of 450, 330, and 280. Each image is dimensionless in the entire visualized area with film half-widths in the streamwise direction and spanwise direction, respectively. In Fig. 2 (a), the entire flow has a light/dark pattern, so the overall flow condition is turbulent. In Fig. 2 (b), turbulent stripe composed of light/dark turbulent regions, and dark quasi-laminar regions. Turbulent stripes can be seen at a Reynolds number of 330. Turbulent stripe is guided by yellow lines. In Fig. 2 (c), no turbulent stripe is observed, and the flow has a dark pattern, so the overall flow condition is laminar flow. From Fig. 2, turbulent, turbulent stripe, and laminar flow were discriminated. Based on the turbulent stripes in Fig. 2 (b), the turbulent stripes in this study were discriminated.

The *Re* range in which turbulent stripes could be visualized in this study was from 330 to 350, which is consistent with the *Re* range in which turbulent stripes appeared, compared to the report by Manneville *et al*. (2004). The visualization movie at *Re* = 330 shows a coexistence of laminar and turbulent regions, and turbulent stripes appear. At *Re* = 320, the entire flow is in the laminar region. Therefore, the critical Reynolds number in this study is considered to exist between *Re* = 320 and 330. The critical Reynolds number range of this study is consistent with Duguet *et al*. (2010), which reported a critical Reynolds number of $Re = 324 \pm 1$ in their numerical simulation of a plane Couette flow. Table 1 shows the Reynolds number range in which turbulent stripes were observed and the angle of the turbulent stripes with against the streamwise direction, with the reports of previous studies (Barkley *et al*., 2005; Tsukahara *et al*., 2010). The plane Couette flow and the plane Poiseuille flow are denoted by PCF and PPF, respectively, and the angle of the turbulent stripe with respect to the streamwise direction is defined by θ. One turbulent band of $\theta = 20^\circ$, 35° and 37° was observed at *Re* = 330 in this study. The angle of the turbulent stripe was consistent with $\theta = 21^\circ$ in Tsukahara *et al*. (2010). Barkley *et al*. (2005) reported $\theta = 37^\circ$ at *Re* = 340, which is in alignment with the value of $\theta = 35^\circ$, 37° found in this study. The angle of the turbulent stripe in the PCF and PPF of the previous study and the value of the present study are consistent, suggesting that the angle is independent of the PCF and PPF. In previous studies, the value of θ tends to decrease as the Reynolds number increases. However, in the present study, turbulent stripes of $\theta = 20^\circ$, 35° and 37° appeared at *Re* = 330, suggesting that the angle of the PCF turbulent stripes is independent of the value of the Reynolds number.

Two patterns of cycles of turbulent stripe appearance and decay existed at *Re* = 330 in this study. The cycles were named long-life cycle (Fig. 3) and short-life cycle (Fig. 4) in the order of appearance. Turbulent stripes are guided by yellow lines. Here, $\Delta t^*(= U_w \Delta t/\delta)$ is the time elapsed since the start of observation, which is non-dimensionalized by the film velocity and film half width. At $\Delta t^* = 7700$ (Fig. 3 (a)), a turbulent stripe with an angle of 20° across the entire stremwise direction appeared on the lower side of the spanwise direction. At $\Delta t^* = 8510$ (Fig. 3 (b)), a turbulent stripe with an angle of 35° appeared on the upper side of the spanwise direction at the same time as the turbulent stripe that appeared decayed. The turbulent stripe appearing at $\Delta t^* = 8510$ (Fig. 3 (b)) sustains, and at $\Delta t^* = 10500$ (Fig. 3 (d)) the turbulent stripe diminished to exist throughout the flow. From the above, the survival time of the turbulent stripe was $t^* = 1960$ with $\theta = 35^\circ$.

A space-diagram with a long-life cycle of $\delta = 3.39$ mm was created to capture the temporal variation of large turbulent stripes. A row of pixels (1.10 mm wide) at approximately 80 δ upstream from the streamwise direction was combined in chronological order from left to right. The space-diagram for a long-life cycle of *Re* = 330 is shown in Fig. 5. The vertical axis is spanwise and the horizontal axis is time, both of which are non-dimensionalized. In Fig. 5, turbulent stripe appears in the lower spanwise direction from $\Delta t^* = 7700$ to $\Delta t^* = 8510$, when the long-life cycle is confirmed, and the space-diagram shows that the structure of turbulent stripe guided by yellow lines is sustained until $\Delta t^* = 8510$. Then, at $\Delta t^* = 8510$, the turbulent stripe on the lower side of the spanwise direction decays, and another turbulent stripe appears on the upper side. The newly emerged turbulent stripe sustained its structure until the end of the long-life cycle.

Figure 4 shows the short-life cycle. At $\Delta t^* = 11300$ (Fig. 4 (a)), one turbulent band of 37° appeared at the center of the visualization area. At $\Delta t^* = 12200$ (Fig. 4 (b)) the turbulent stripe split into two guided by yellow circles. However, at $\Delta t^* = 12300$ (Fig. 4 (c)), the split turbulent regions remerged and returned to their original shape. Thereafter, the turbulent stripe structure sustained, and at $\Delta t^* = 12600$ (Fig. 4 (d)) the turbulent stripe diminished to exist throughout the flow. The survival time of the turbulent stripe was $t^* = 1240$ with $\theta = 37^\circ$.

Comparing each cycle with $\delta = 3.39$ mm, turbulent stripes with longer survival times appeared in the long-life cycles.

Both long-life and short-life cycles visualized at one turbulence stripe in the visualization area, and the angle was not different in each cycle.

CHARACTERISTICS OF FIVE TURBULENT BANDS

Long-life and short-life cycles were also observed at Re = 300 for δ = 2.90 mm. Figure 6 shows long-life cycle from the appearance of the turbulent stripe to its decay at Re = 300. Turbulent stripes are guided by yellow lines. At Δt^* = 162 (Fig. 6 (a)), a turbulent stripe with θ = 40° appeared downstream, and at Δt^* = 616 (Fig. 6 (b)), a turbulent stripe with θ = 40° was visualized, which was opposite to the angle of turbulent stripe in Fig. 6 (a). At Δt^* = 681 (Fig. 6 (c)), the turbulent stripe in Fig. 6 (b) was mixed with the upstream turbulent region and decayed. Then, at Δt^* = 1780, the turbulent stripe surviving since the beginning of the observation decayed, and at Δt^* = 1910 (Fig. 6 (d)), the turbulent stripe diminished to exist throughout the visualized flow. From the above, the survival time of the turbulent stripe was t^* = 819 with θ = 20° and t^* = 1620 with θ = 40°.

Figure 7 shows short-life cycle from the appearance of the turbulent stripe to its decay at Re = 300. At Δt^* = 2110 in Fig. 7 (a), two turbulent bands with θ = 0° and one turbulent band with θ = 20° appeared downstream. One turbulent band with θ = 0° flowed upstream and decayed, while the other one mixed with the surrounding turbulent region. Three turbulent bands with θ = 0° appeared downstream and upstream of the spanwise direction at Δt^* = 2760 in Fig. 7 (c), and five turbulent bands were visualized in the entire flow. This was the largest number of turbulent bands visualized in the flow at Re = 300 of Δt^* = 2760 in this study. At Δt^* = 2890 in Fig. 7 (d), two turbulent bands with θ = 0° decayed. At Δt^* = 3080, two turbulent bands with θ = 20° decayed, and at Δt^* = 3690, turbulent stripes diminished to exist in the entire flow as in Fig. 7 (d). From the above, the survival time of the turbulent stripe was t^* = 970 with θ = 20°. The case of the decay of the turbulent stripe with θ = 0° at t^* = 162. Fukudome *et al.* (2013) reported that collision between high-and-low-speed streaks does not occur when the turbulent region exists parallel to the streamwise direction. Onishi *et al.* (2010) reported that the collision between high-and-low-speed streaks is essential for the generation and maintenance of turbulent stripes, which may be the reason why the θ = 0° of turbulent stripe observed in this study decayed in a short time.

Comparing the two cycles for δ = 2.90 mm, the survival time of turbulent stripe of θ = 40° in long-life cycle was t^* = 1620, whereas the survival time of θ = 20° turbulent stripe in short-life cycle was t^* = 970. Duguet *et al.* (2010) reported that an angle close to θ = 40° was most likely to appear in the early stage of turbulent stripe development, which was consistent with this experiment. The survival time of the turbulent stripe at θ = 40° was the longest, suggesting that the energy cycle of the turbulent stripe was stably supplied at θ = 40°.

RELATIONSHIP BETWEEN ASPECT RATIO AND THE NUMBER OF TURBULENT BANDS

The Re range, in which the turbulent stripe was visualized at δ = 2.90 mm, was within 300 and 350. It is a little lower than the Re range at δ = 3.39 mm in this study and that reported by Manneville (2004). However, since the standard deviation of δ in this study are 0.26 mm, the Re range where the turbulent stripe appears are consistent with previous study. Five turbulent bands with θ = 0° and two turbulent bands with θ = 20°, 40° were observed, respectively, during 114 s imaging at Re = 300 in this study. Turbulent stripes with θ = 0° appeared most frequently, and those with θ = 20° and 40° appeared at the same frequency.

Here, the turbulent fraction for the experimental results for each δ were determined and compared with those reported by Duguet *et al.* (2010). In this study, the turbulent fraction, which indicates the percentage of turbulent areas within the visualized area, was defined by the percentage of white areas (turbulent areas) in the image after morphology processing after binarization of the image. The turbulent fraction was followed for 120 s, and remained constant at each Reynolds number, regardless of the appearance or absence of turbulent stripes. Figure 8 shows the intermittency calculated by time averaging at 120 s for each Reynolds number of squares (large δ), and diamond (small δ). The turbulent fraction reported by Duguet *et al.* (2010) by direct numerical simulation is shown in circles. Duguet *et al.* (2010) obtained the turbulent fraction from the percentage of regions with turbulence generation above a certain threshold, which is strictly different from the turbulent fraction defined in this study. The measured turbulent fraction of large δ is almost identical to that reported by Duguet *et al.* (2010). The trend in this study of decreasing the turbulent fraction from Re = 380 as the Reynolds number is decreased from Re = 450 is consistent with the decreasing rate of turbulent fraction (Duguet *et al.*, 2010). Numerical simulation has shown that the turbulent fraction of the plane Couette flow has two types of slopes: one is a gradual decrease in value as the Reynolds number is lowered from turbulent fraction, and the other is a sharp decrease in turbulent fraction from a certain Reynolds number. This experiment of each δ was able to confirm both a gradual and a sharp decrease in the turbulent fraction. The difference between the maximum and minimum values of the turbulent fraction (ΔRe) and the critical Reynolds number (Re_{cr}) were obtained by applying the sigmoid function to the turbulent fraction values of Duguet *et al.* (2010) and present study. For large δ, ΔRe was 0.20, for small δ, it was 0.18, and for Duguet et al. (2010), it was 0.22. For large δ, Re_{cr} was 0.67, for small δ, it was 0.63, and for Duguet et al. (2010), it was 0.60. For small δ, the increase in the turbulent fraction rate occuered earlier than in the other two results, but both ΔRe and Re_{cr} showed similar values. there is no difference between the experimental and numerical results for the turbulent fraction.

The long-life and short-life cycles are compared for each film half-width δ = 2.90 and 3.39 mm. The angle and number of turbulent bands, appearing in the long-life cycle, was 40° for δ = 2.90 mm, with two turbulent bands visualized. And 35° for δ = 3.39 mm, with one turbulent band was visualized. While relatively similar angles could be identified, the number of turbulent bands in the entire flow was much for δ = 2.90 mm. The angle and number of turbulent bands appearing in the short-life cycle were 0° for δ = 2.90 mm, and five turbulent bands were visualized at 20°. At 37° with δ = 3.39 mm, a maximum of one turbulent band was visualized throughout the flow. Regarding the angles of the turbulent stripes observed in the short-life cycle, the angle at δ = 3.39 mm was about twice as large as the angle appearing at δ = 2.90 mm. As with the long-life cycles, the number of turbulent bands, that appeared in the entire flow, was much for δ = 2.90 mm.

The difference in the angle and number of turbulent bands is considered to be caused by the film half-width. Table 2 compares the values of this study with those reported from experiments in which turbulent stripes were visualized at different film half-widths. Comparison is made in terms of visible area, film half-width, number of turbulent bands, and spanwise wavelength (λ_z); Yimprasert *et al.* (2021) reported λ_z/δ = 188 and one turbulent band at δ = 3.50. This study identified one turbulent band with δ = 3.50 of λ_z/δ = 31.7, and five turbulent bands with δ = 2.90 of λ_z/δ = 24. Prigent *et al.* (2005) reported λ_z/δ = 21.1 and five turbulent bands at δ = 1.50. Experiments conducted in this study with different film half-widths resulted in larger number of turbulent bands and smaller values of spanwise wavelength for the small δ. It is difficult to say that it cannot be organized by δ because the standard deviation of the film half-width is 0.26 mm for small δ and 0.27 mm for large δ. The same order of spanwise wavelengths can also be assumed from the report by Duguet *et al.* (2013) that non-dimensionalized the spanwise wavelengths by δ. On the other hand, Tsukahara *et al.* (2010) reported that the value of spanwise wavelength decreases as the value of Re_τ increases in PPF and PCF. From this study and Tsukahara *et al.*'s report, spanwise wavelengths are considered to be organized on a viscous scale. Thus, future works need inclusion of discussion about the influence of δ on turbulent bands.

CONCLUSION

In this study, the spatio-temporal variation of turbulent stripes in the plane Couette flow was investigated. The findings are summarized as follows.

- Two cycles of turbulent stripe appearance and decay were filmed in the transition region of a plane Couette flow, and differences in the angle (θ) and number of turbulent bands existed in each cycle. The survival time of turbulent stripes was found to be longer in the first long-life cycle that appeared than in the second short-life cycle.
- In the short-life cycle at Reynolds number of 300, a maximum of five turbulence bands were visualized in the flow, and the survival time of turbulent stripe with $\theta = 40^\circ$ was the longest compared to stripes at other angles at $t^* = 1620$, which was non-dimensionalized by the film velocity and film half-width (δ). At $Re = 330$, the survival time of turbulent stripe with $\theta = 35^\circ$ was the longest in this study. Based on the results of turbulent stripe with survival time, the angle, at which turbulent stripes are stable in plane Couette flow experiments, are considered to be the range is 35° and 40°.
- The experimental results in this study showed that the value of spanwise wavelength was different for small and large δ.

REFERENCES

Barkley, D. & Tuckerman, L. S. 2005 Turbulent-laminar patterns in plane couette flow. In *IUTAM Symposium on Laminar-Turbulent Transition and Finite Amplitude Solutions*, pp. 107–127.

Couliou, M. & Monchaux, R. 2015 Large-scale flows in transitional plane couette flow: a key ingredient of the spot growth mechanism. *Physics of Fluids* **27** (3), 034101.

Duguet, Y., Monokrousos, A., Brandt, L. & Henningson, D. S. 2013 Minimal transition thresholds in plane couette flow. *Physics of Fluids* **25** (8), 084103.

Duguet, Y., Schlatter, P. & Henningson, D. S. 2010 Formation of turbulent patterns near the onset of transition in plane couette flow. *Journal of Fluid Mechanics* **650**, 119–129.

Fukuda, T. & Tsukahara, T. 2020 Heat transfer of transitional regime with helical turbulence in annular flow. *International Journal of Heat and Fluid Flow* **82**, 108555.

Fukudome, K. & Iida, O. 2013 Effect of large-scale structure generated in low-reynolds-number poiseuille flow on longitudinal vortices. *Transactions of the Japan Society of Mechanical Engineers. Series B* **79** (807), 2352–2362 (in Japanese).

Fukudome, K. & Ogami, Y. 2015 On the scale and angular dependence of large-scale intermittent structures in lowreynolds-number interplanar flows. *RIMS* **1944**, 15–23 (in Japanese).

Fukudome, K., Tsukahara, T. & Ogami, Y. 2018 Heat and momentum transfer of turbulent stripe in transitional-regime plane couette flow. *International Journal of Advances in Engineering Sciences and Applied Mathematics* **10** (4), 291–298.

Gomé, S., Tuckerman, L, S. & Barkley, D. 2020 Statistical transition to turbulence in plane channel flow. *Physical Review Fluids* **5** (8), 083905.

Hashimoto, S., Hasobe, A., Tsukahara, T., Kawaguchi, Y. & Kawamura, H. 2009 An experimental study on turbulent-stripe structure in transitional channel flow. In *ICHMT DIGITAL LIBRARY ONLINE*. Begel House Inc.

Manneville, P. 2004 Spots and turbulent domains in a model of transitional plane couette flow. *Theoretical and Computational Fluid Dynamics* **18** (2-4), 169–181.

Ohnishi, K., Tsukahara, T. & Kawaguchi, Y. 2011 Turbulence budget in transitional plane couette flow with turbulent stripe. In *Journal of Physics: Conference Series*, , vol. 318, pp. 32–33.

Paranjape, C. S., Duguet, Y. & Hof, B. 2020 Oblique stripe solutions of channel flow. *Journal of Fluid Mechanics* **897**, A7.

Prigent, A. & Dauchot, O. 2005 Transition to versus from turbulence in subcritical couette flows. In *IUTAM Symposium on Laminar-Turbulent Transition and Finite Amplitude Solutions*, pp. 195–219.

Prigent, A., Grégoire, G., Chaté, H. & Dauchot, O. 2003 Long-wavelength modulation of turbulent shear flows. *Physica D: Nonlinear Phenomena* **174** (1-4), 100–113.

Reetz, F., Kreilos, T. & Schneider, T. M. 2019 Exact invariant solution reveals the origin of self-organized oblique turbulent-laminar stripes. *Nature Communications* **10** (1), 1–6.

Tsukahara, T., Kawaguchi, Y., Kawamura, H., Tillmark, N. & Alfredsson, P. H. 2010 Turbulence stripe in transitional channel flow with/without system rotation. In *Seventh IUTAM Symposium on Laminar-Turbulent Transition*, pp. 421–426.

Yimprasert, S., Kvick, M., Alfredsson, P, H. & Matsubara, M. 2021 Flow visualization and skin friction determination in transitional channel flow. *Experiments in Fluids* **62** (2), 1–16.

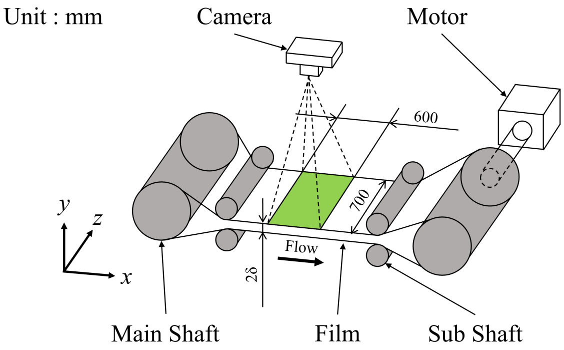

Figure 1: Schematic view of the experiment set-up. Flow is left to right. The captured area by the camera is the green. Experiments were conducted with different film half-widths (large δ, small δ).

Table 1: Reynolds number at which the turbulent stripe appeared and the angle of the turbulent stripe with respect to the flow direction (θ) were compared.

	Flow	*Re*	θ (deg)
Barkley *et al.* (2005)	PCF	340	37
		394	25
Tsukahara *et al.* (2010)	PCF	350	27
		375	27
	PPF	268	21
		293	21
Present	PCF	330 - 350	20 - 37

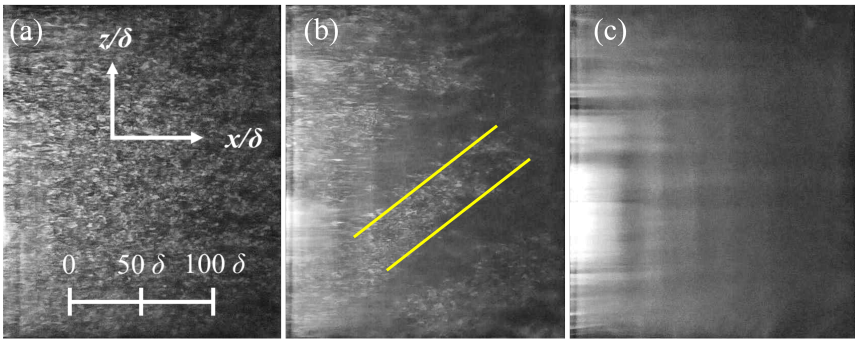

Figure 2: Flow visualization of plane Couette flow. (a)All captured area is turbulent at Re = 450; (b)Visualization of turbulent stripes guided by yellow at Re = 330; (c)All captured area is laminar flow at Re = 280. The captured area is of 600 mm $\times$ 700 mm.

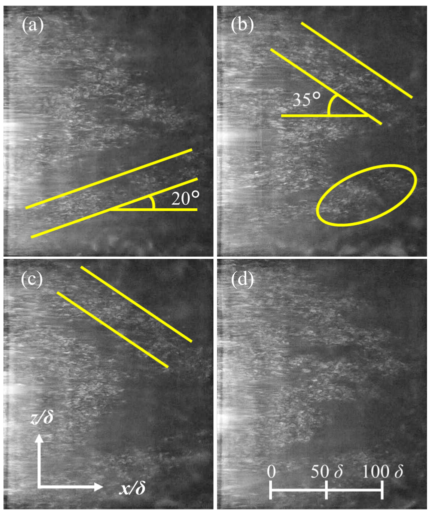

Figure 3: Long-life cycle of turbulent stripes that appear and then decay at Re = 330. (a)Δt^* = 7700; (b)Δt^* = 8510; (c)Δt^* = 9430; (d)Δt^* = 10500.

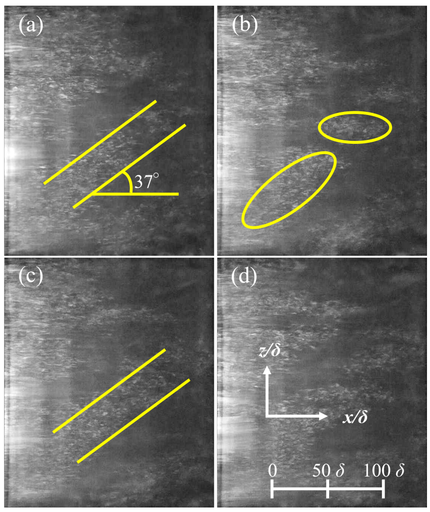

Figure 4: Short-life cycle of turbulent stripes that appear and then decay at Re = 330. (a)Δt^* = 11300; (b)Δt^* = 12200; (c)Δt^* = 12300; (d)Δt^* = 12600.

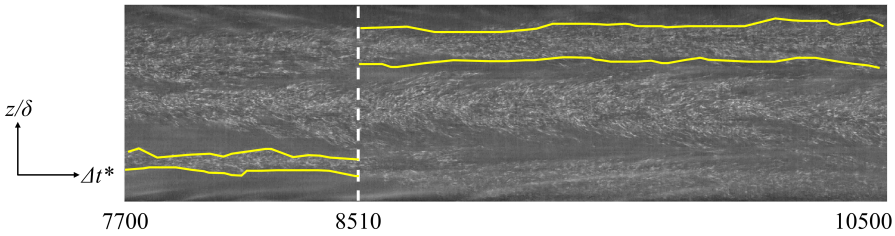

Figure 5: Space-diagram of the long-life cycle at Re = 330. The white dashed line shows that the decay and turbulent stripes occur almost simultaneously.

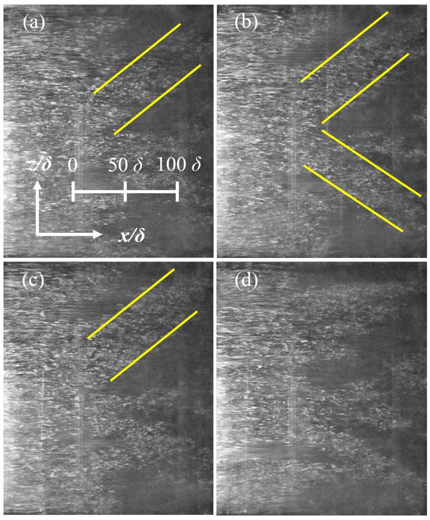

Figure 6: Long-life cycle of turbulent stripes that appear and then decay at Re = 300. (a)Δt^* = 162; (b)Δt^* = 616; (c)Δt^* = 681; (d)Δt^* = 1910.

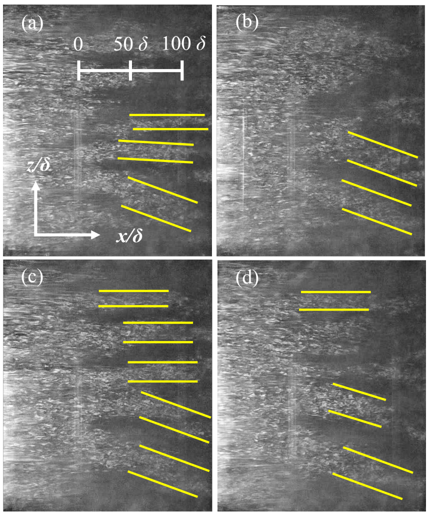

Figure 7: Short-life cycle of turbulent stripes that appear and then decay at Re = 300. (a)Δt^* = 2110; (b)Δt^* = 2370; (c)Δt^* = 2760; (d)Δt^* = 2890.

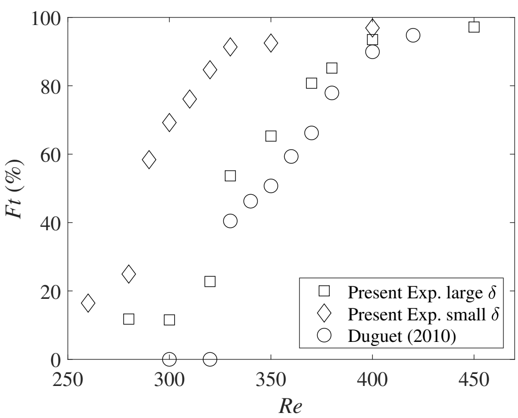

Figure 8: Turbulent fraction at time average of each Reynolds number.

Table 2: Differences in the spanwise wavelength (λ_z), and number of bands of turbulent stripes across the film half-width.

	δ	bands	λ_z/δ	$x/\delta \times z/\delta$	Flow
Yimprasert *et al.* (2021)	3.50	1	188	1330 × 166	PPF
Present study	3.39	1	31.7	177 × 206	PCF
	2.90	5	24.0	207 × 241	
Prigent *et al.* (2005)	1.50	5	21.1	385 × 169	PCF